Available online at www.sciencedirect.com
SCIENCE DIRECT®
ELSEVIER
Topology and its Applications 152 (2005) 157–173
Topology and its Applications
www.elsevier.com/locate/topol

Analytical 3-dimensional anisotropic plasma equilibria

Alexei F. Cheviakov

Department of Mathematics and Statistics, Queen's University, Kingston K7L 3N6, Canada

Received 15 October 2003; received in revised form 21 July 2004

Abstract

In this paper we present a method of constructing a wide class of analytical solutions to Anisotropic Plasma Equilibrium equations in Chew–Goldberger–Low (CGL) approximation.

The method is based on an explicit infinite-dimensional set of transformations between solutions of isotropic Magnetohydrodynamic (MHD) equilibrium equations and solutions of CGL equilibrium equations. These transformations depend on the topology of the original solution and allow the building anisotropic plasma equilibria with a variety of physical properties and topologies, including 3D solutions with no geometrical symmetries.

Anisotropic plasma equilibrium configurations with and without magnetic surfaces can be built using these transformations. The examples are given.

PACS: 52.30.Cv; 05.45.-a; 02.30.Jr; 02.90.+p

Keywords: MHD; Plasma; Anisotropic; Analytic; Equilibrium

1. Introduction

The two most commonly used single-fluid models of plasma as a continuous medium are the isotropic magnetohydrodynamics (MHD) equations [1] and the anisotropic CGL (Chew–Goldberger–Low) magnetohydrodynamics equations [2].

E-mail address: alexch@mast.queensu.ca (A.F. Cheviakov).

0166-8641/$ – see front matter
doi:10.1016/j.topol.2004.08.020

These systems are used to model phenomena in different areas of physics—controlled thermonuclear fusion studies [1,3], astrophysical problems (star formation, solar activity, astrophysical jets) [4–8], terrestrial applications (laboratory and industrial plasmas, ball lightning models) [9–13].

The isotropic MHD approximation was derived from Boltzmann and Maxwell equations under the assumption that the mean free path of plasma particles is much less than the typical scale of the task, therefore the picture is maintained nearly isotropic via frequent collisions. The system of equations of MHD system is

$$\begin{aligned}
&\rho\partial\mathbf{V}/\partial t = \rho\mathbf{V}\times\operatorname{curl}\mathbf{V} - \frac{1}{\mu}\mathbf{B}\times\operatorname{curl}\mathbf{B} - \operatorname{grad}P - \rho\operatorname{grad}\frac{\mathbf{V}^2}{2} + \nu_k\cdot\nabla^2\mathbf{V},\\
&\partial\mathbf{B}/\partial t = \operatorname{curl}(\mathbf{V}\times\mathbf{B}) + \nu_m\cdot\nabla^2\mathbf{B}, \qquad \nu_m = \frac{1}{\sigma\mu},\\
&\partial\rho/\partial t + \operatorname{div}\rho\mathbf{V} = 0, \qquad \operatorname{div}\mathbf{B} = 0.
\end{aligned} \tag{1}$$

Here $\mathbf{V}$ is plasma velocity; $\mathbf{B}$ is the vector of the magnetic field induction; ρ, plasma density; P, scalar plasma pressure; ν_k, kinetic viscosity; ν_m, magnetic viscosity; σ, electrical conductivity; and μ, magnetic permeability coefficient.

When the mean free path for particle collisions is long compared to Larmor radius, for instance, in strongly magnetized or rarified plasmas, the CGL approximation with tensor pressure $\mathbb{P}$ should be used. The pressure tensor has two different components: the pressure along the magnetic field $p_\parallel$ and in the transverse direction $p_\perp$. In the limit $p_\perp = p_\parallel = p$, CGL and MHD models coincide.

The CGL system has the form

$$\begin{aligned}
&\rho\partial\mathbf{V}/\partial t = \rho\mathbf{V}\times\operatorname{curl}\mathbf{V} - \frac{1}{\mu}\mathbf{B}\times\operatorname{curl}\mathbf{B} - \operatorname{div}\mathbb{P} - \rho\operatorname{grad}\frac{\mathbf{V}^2}{2} + \nu_k\cdot\nabla^2\mathbf{V},\\
&\partial\mathbf{B}/\partial t = \operatorname{curl}(\mathbf{V}\times\mathbf{B}) + \nu_m\cdot\nabla^2\mathbf{B}, \qquad \nu_m = \frac{1}{\sigma\mu},\\
&\partial\rho/\partial t + \operatorname{div}\rho\mathbf{V} = 0, \qquad \operatorname{div}\mathbf{B} = 0.
\end{aligned} \tag{2}$$

The MHD system (1) must be extended with a single equation of state to make it closed, whereas the set of CGL equations (2) needs two equations of state, or one equation of state and one equation connecting the pressure components. The original work by Chew, Goldberger and Low contains two adiabatic laws [2], which have been obtained in the assumption of vanishing of the pressure-transport tensor:

$$\frac{\mathrm{d}}{\mathrm{d}t}\left(\frac{p_\perp}{\rho B}\right) = 0, \qquad \frac{\mathrm{d}}{\mathrm{d}t}\left(\frac{p_\parallel B^2}{\rho^3}\right) = 0. \tag{3}$$

However, experimental measurements of anisotropic plasmas yield different empirical relations. For example, in the studies of the solar wind flow in the Earth magnetosheath, the relation

$$p_\perp/p_\parallel = 1 + 0.847\big(B^2/(2p_\parallel)\big) \tag{4}$$

is proposed [14]. In the Compact Helical System (CHS) plasma confinement device, the anisotropy factors $p_\parallel/p_\perp \propto 3$ have been measured [15].

In many applications, equilibrium plasma flows and static configurations are of particular interest. Current paper is devoted to the analytical study of such configurations in isotropic and anisotropic cases.

The system of MHD equilibrium equations, under the assumptions of infinite conductivity and negligible viscosity, is found from the time-dependent system (1) to be

$$\rho\mathbf{V}\times\operatorname{curl}\mathbf{V}-\frac{1}{\mu}\mathbf{B}\times\operatorname{curl}\mathbf{B}-\operatorname{grad}P-\rho\operatorname{grad}\frac{\mathbf{V}^2}{2}=0, \tag{5}$$

$$\operatorname{div}\rho\mathbf{V}=0,\qquad \operatorname{curl}(\mathbf{V}\times\mathbf{B})=0,\qquad \operatorname{div}\mathbf{B}=0. \tag{6}$$

For anisotropic plasma equilibria are described by time-independent Chew–Goldberger–Low equations

$$\rho\mathbf{V}\times\operatorname{curl}\mathbf{V}-\frac{1}{\mu}\mathbf{B}\times\operatorname{curl}\mathbf{B}=\operatorname{div}\mathbb{P}+\rho\operatorname{grad}\frac{\mathbf{V}^2}{2}, \tag{7}$$

$$\operatorname{div}\rho\mathbf{V}=0,\qquad \operatorname{curl}(\mathbf{V}\times\mathbf{B})=0,\qquad \operatorname{div}\mathbf{B}=0, \tag{8}$$

where $\mathbb{P}$ is the pressure tensor with two independent components:

$$\mathbb{P}=\mathbb{I}p_\perp+\frac{p_\parallel-p_\perp}{\mathbf{B}^2}(\mathbf{BB}). \tag{9}$$

Here $\mathbb{I}$ is a unit tensor.

In Section 2 of the current paper we present a new *infinite-dimensional* set of transformations between isotropic (MHD) and anisotropic (CGL) plasma equilibria. These transformations can be applied to any static plasma equilibrium and to a wide class of dynamic equilibria to yield physically interesting anisotropic equilibrium solutions.

The topology of the original isotropic plasma equilibrium is essential for the transformations. It is well known that all isotropic nonviscous incompressible MHD equilibria (except Beltrami flows) have a special topology—the plasma domain is spanned by nested 2-dimensional *magnetic surfaces*—surfaces on which magnetic field lines and plasma streamlines lie [16–19]. The new transformations explicitly depend on two arbitrary functions constant on magnetic surfaces (or constant on magnetic field lines and plasma streamlines, if the magnetic surfaces seize to exist.) The arbitrary functions are therefore generally functions on a *cellular complex*.

In Section 3 we discuss necessary physical conditions that isotropic and anisotropic plasma equilibria must satisfy to be physically relevant. We show that the new transformations often allow the building of anisotropic plasma equilibria satisfying the physical conditions and stable with respect to fire-hose and mirror instabilities.

Using the new transformations, we build several analytical examples of localized and nonlocalized anisotropic plasma equilibria with different pressure profiles and different topologies.

In Section 4, we give examples of building a closed nonsymmetric anisotropic plasma flux tube (Section 4.1), a plasma configuration with no magnetic surfaces (Section 4.2), and the model of anisotropic astrophysical jets (Section 4.3).

The new transformations can be successfully applied to other known analytical isotropic MHD models, such as the Ball lightning model of Kaiser and Lortz [10], to produce corresponding anisotropic plasma equilibria with the same topology.

2. Transformations between MHD and CGL equilibria

The equilibrium states of isotropic moving plasmas are described by the system of MHD equilibrium equations, which under the assumptions of infinite conductivity and negligible viscosity has the form (5), (6).

In the case of incompressible plasma, the equation

$$\operatorname{div}\mathbf{V} = 0 \tag{10}$$

is added to the above system; for a compressible case an appropriate equation of state must be chosen. For example, it can be the adiabatic ideal gas equation of state:

$$P = \rho^{\gamma}\exp(S/c_v), \qquad \mathbf{V}\cdot\operatorname{grad} S = 0. \tag{11}$$

Here c_v is the heat capacity at constant volume; γ, the adiabatic exponent; and S, entropy.

In this paper we restrict our consideration to incompressible plasmas. Incompressibility condition is widely used in MHD studies. For example, it is a good approximation for subsonic plasma flows with low Mach numbers $M \ll 1$, $M^2 = \mathbf{V}^2/(\gamma P/\rho)$. For incompressible plasma the continuity equation $\operatorname{div}\rho\mathbf{V} = 0$ implies $\mathbf{V}\cdot\operatorname{grad}\rho = 0$, hence density is constant on plasma streamlines.

It is known [16–19] that all compact incompressible MHD equilibrium configurations, except the Beltrami case $\operatorname{curl}\mathbf{B} = \alpha\mathbf{B}$, $\alpha = \text{const}$, possess two-dimensional magnetic surfaces—the vector fields $\mathbf{B}$ and $\mathbf{V}$ are in every point tangent to magnetic surfaces. The magnetic surfaces may not exist for unbounded incompressible MHD equilibrium configurations with $\mathbf{V} \parallel \mathbf{B}$.

For *anisotropic* nonviscous plasmas with Larmor radius small compared to characteristic dimensions of the system, the corresponding set of equations was found by Chew, Goldberger and Low and has the form (7), (8).

For this system to be closed, one needs to add to it two equations of state. In this chapter we will consider incompressible CGL plasmas: $\operatorname{div}\mathbf{V} = 0$.

Using vector calculus identities, the divergence of the pressure tensor may be rewritten in the form

$$\operatorname{div}\mathbb{P} = \operatorname{grad} p_{\perp} + \tau\operatorname{curl}\mathbf{B}\times\mathbf{B} + \tau\operatorname{grad}\frac{\mathbf{B}^2}{2} + \mathbf{B}(\mathbf{B}\cdot\operatorname{grad}\tau), \tag{12}$$

$$\tau = \frac{p_{\parallel} - p_{\perp}}{\mathbf{B}^2}. \tag{13}$$

Hence the system (7), (8) rewrites as

$$\begin{aligned}\rho\mathbf{V}\times\operatorname{curl}\mathbf{V} - \left(\frac{1}{\mu} - \tau\right)\mathbf{B}\times\operatorname{curl}\mathbf{B}\\ = \operatorname{grad} p_{\perp} + \rho\operatorname{grad}\frac{\mathbf{V}^2}{2} + \tau\operatorname{grad}\frac{\mathbf{B}^2}{2} + \mathbf{B}(\mathbf{B}\cdot\operatorname{grad}\tau),\end{aligned} \tag{14}$$

$$\operatorname{div}\mathbf{V} = 0, \qquad \operatorname{div}\mathbf{B} = 0, \qquad \operatorname{curl}(\mathbf{V}\times\mathbf{B}) = 0. \tag{15}$$

The following theorem shows that there exist infinite-dimensional transformations that map solutions of incompressible MHD equilibrium equations to incompressible anisotropic (CGL) equilibria.

Theorem 1. *Let* $\{\mathbf{V}(\mathbf{r}), \mathbf{B}(\mathbf{r}), P(\mathbf{r}), \rho(\mathbf{r})\}$ *be a solution of the system* (5)–(10) *of incompressible MHD equilibrium equations, where the density* $\rho(\mathbf{r})$ *is constant on both magnetic field lines and streamlines* (*i.e., in magnetic surfaces* $\Psi = \text{const}$, *if they exist.*)

Then $\{\mathbf{V}_1(\mathbf{r}), \mathbf{B}_1(\mathbf{r}), p_{\perp 1}(\mathbf{r}), p_{\parallel 1}(\mathbf{r}), \rho_1(\mathbf{r})\}$ *is a solution to incompressible CGL plasma equilibria* (14), (15), *where*

$$\begin{aligned}
&\mathbf{B}_1(\mathbf{r}) = f(\mathbf{r})\mathbf{B}(\mathbf{r}), \qquad \mathbf{V}_1(\mathbf{r}) = g(\mathbf{r})\mathbf{V}(\mathbf{r}), \qquad \rho_1 = C_0\rho(\mathbf{r})\mu/g(\mathbf{r})^2,\\
&p_{\perp 1}(\mathbf{r}) = C_0\mu P(\mathbf{r}) + C_1 + \big(C_0 - f(\mathbf{r})^2/\mu\big)\mathbf{B}(\mathbf{r})^2/2,\\
&p_{\parallel 1}(\mathbf{r}) = C_0\mu P(\mathbf{r}) + C_1 - \big(C_0 - f(\mathbf{r})^2/\mu\big)\mathbf{B}(\mathbf{r})^2/2,
\end{aligned} \tag{16}$$

and $f(\mathbf{r})$, $g(\mathbf{r})$ *are arbitrary functions constant on the magnetic field lines and streamlines.* C_0, C_1 *are arbitrary constants.*

Proof. Let us insert the quantities (16) into the system of CGL plasma equilibrium equations (14), (15), assuming that $\{\mathbf{V}(\mathbf{r}), \mathbf{B}(\mathbf{r}), P(\mathbf{r}), \rho(\mathbf{r})\}$ is an isotropic MHD equilibrium and satisfies (5), (6), (10).

To simplify the notation, we do not write the dependence of functions on $\mathbf{r}$ explicitly.

The functions $f(\mathbf{r})$, $g(\mathbf{r})$ are constant on the magnetic field lines and streamlines, therefore

$$\begin{aligned}
&\operatorname{div}\mathbf{B}_1 = f\operatorname{div}\mathbf{B} + \mathbf{B}\operatorname{grad} f = 0,\\
&\operatorname{div}\mathbf{V}_1 = g\operatorname{div}\mathbf{V} + \mathbf{V}\operatorname{grad} g = 0.
\end{aligned} \tag{17}$$

Also, using a vector calculus identity

$$\operatorname{curl}(s\mathbf{q}) = s\operatorname{curl}\mathbf{q} + \operatorname{grad}(s)\times\mathbf{q}, \tag{18}$$

we conclude that

$$\operatorname{curl}(\mathbf{V}_1\times\mathbf{B}_1) = 0, \tag{19}$$

therefore equations (15) are satisfied.

To prove that (14) holds, we first observe that

$$\begin{aligned}
&\rho_1\mathbf{V}_1\times\operatorname{curl}\mathbf{V}_1 - \left(\frac{1}{\mu} - \tau_1\right)\mathbf{B}_1\times\operatorname{curl}\mathbf{B}_1\\
&\quad= \rho_1 g^2\mathbf{V}\times\operatorname{curl}\mathbf{V} - \left(\frac{1}{\mu} - \tau_1\right)f^2\mathbf{B}\times\operatorname{curl}\mathbf{B}\\
&\qquad + \mathbf{V}^2\rho_1 g\operatorname{grad}(g) - \mathbf{B}^2\left(\frac{1}{\mu} - \tau_1\right)f\operatorname{grad}(f)\\
&\quad= C_0\mu\left(\rho\mathbf{V}\times\operatorname{curl}\mathbf{V} - \frac{1}{\mu}\mathbf{B}\times\operatorname{curl}\mathbf{B}\right)\\
&\qquad + \mathbf{V}^2\rho_1 g\operatorname{grad}(g) - \mathbf{B}^2\left(\frac{1}{\mu} - \tau_1\right)f\operatorname{grad}(f)\\
&\quad= C_0\mu\left(\operatorname{grad}P + \rho\operatorname{grad}\frac{\mathbf{V}^2}{2}\right) + \mathbf{V}^2\rho_1 g\operatorname{grad}(g) - \mathbf{B}^2\left(\frac{1}{\mu} - \tau_1\right)f\operatorname{grad}(f)
\end{aligned}$$

$$= C_0\mu \operatorname{grad} P + C_0\rho\mu \operatorname{grad} \frac{\mathbf{V}^2}{2} + \frac{C_0\rho\mu\mathbf{V}^2}{2g^2} \operatorname{grad} g^2 - \frac{\mathbf{B}_1^2}{2} \operatorname{grad}(\tau_1).$$

Noting that τ_1 is constant on both magnetic field lines and streamlines, we have

$$\mathbf{B}_1 \cdot \operatorname{grad} \tau_1 = 0.$$

The right-hand side of (14) is

$$\begin{aligned}
&\operatorname{grad} p_{\perp 1} + \rho_1 \operatorname{grad} \frac{\mathbf{V}_1^2}{2} + \tau_1 \operatorname{grad} \frac{\mathbf{B}_1^2}{2} \\
&\quad = \operatorname{grad}\left(p_{\perp 1} + \rho_1 \frac{\mathbf{V}_1^2}{2} + \tau_1 \frac{\mathbf{B}_1^2}{2} \right) - \frac{\mathbf{B}_1^2}{2} \operatorname{grad}(\tau_1) - \frac{\mathbf{V}_1^2}{2} \operatorname{grad}(\rho_1) \\
&\quad = C_0\mu \operatorname{grad} P + C_0\rho\mu \operatorname{grad} \frac{\mathbf{V}^2}{2} + \frac{C_0\rho\mu\mathbf{V}^2}{2g^2} \operatorname{grad} g^2 - \frac{\mathbf{B}_1^2}{2} \operatorname{grad}(\tau_1)
\end{aligned}$$

and is identically equal to the left-hand side. The theorem is proven. □

Remark 1. Under the conditions of the theorem, the anisotropy factor

$$\tau_1 \equiv (p_{\parallel 1} - p_{\perp 1})/\mathbf{B}_1^2 = 1/\mu - C_0/f(\mathbf{r})^2 \tag{20}$$

is also constant on the magnetic field lines and streamlines, and that the following relations hold:

$$\begin{aligned}
p_{\perp 1}(\mathbf{r}) &= C_0\mu P(\mathbf{r}) + C_1 - \tau_1(\mathbf{r})\mathbf{B}_1(\mathbf{r})^2/2, \\
p_{\parallel 1}(\mathbf{r}) &= C_0\mu P(\mathbf{r}) + C_1 + \tau_1(\mathbf{r})\mathbf{B}_1(\mathbf{r})^2/2.
\end{aligned} \tag{21}$$

Remark 2 (*The structure of functions* $f(\mathbf{r})$, $g(\mathbf{r})$). The structure of undefined functions $f(\mathbf{r})$, $g(\mathbf{r})$ in the transformations (16) depends on the topology of the original MHD equilibrium configuration $\{\mathbf{V}(\mathbf{r}), \mathbf{B}(\mathbf{r}), P(\mathbf{r}), \rho(\mathbf{r})\}$.

(i) If the magnetic field $\mathbf{B}$ and velocity $\mathbf{V}$ of the original MHD equilibrium configuration are not collinear, then the vector fields $\mathbf{B}$ and $\mathbf{V}$ are in every point tangent to magnetic surfaces [18,19], and therefore functions $f(\mathbf{r})$, $g(\mathbf{r})$ must be constant on each of these surfaces.

(ii) Magnetic field and velocity are collinear, $\mathbf{B} = k(\mathbf{r})\mathbf{V}$ ($k(\mathbf{r})$ is some smooth function in $\mathbb{R}^3$), and each field line is dense on a 2-dimensional magnetic surface. Then $f(\mathbf{r})$, $g(\mathbf{r})$ have to be constant on every such surface.

(iii) Magnetic field and velocity are collinear, and field lines are closed loops or go to infinity. Then the functions $f(\mathbf{r})$, $g(\mathbf{r})$ only have to be constant on the plasma streamlines.

(iv) Magnetic field and velocity are collinear, and their field lines are dense in some 3D domain $\mathcal{D}$. This situation may only occur if both $\mathbf{B}$ and $\mathbf{V}$ satisfy Beltrami equations $\operatorname{curl}\mathbf{B} = \alpha\mathbf{B}$, $\operatorname{curl}\mathbf{V} = \beta\mathbf{V}$, $\alpha, \beta = \text{const}$. Then the functions $f(\mathbf{r})$, $g(\mathbf{r})$ are constant in $\mathcal{D}$.

Based on this description, we may conclude that the arbitrary functions $f(\mathbf{r})$, $g(\mathbf{r})$ are constant on a cellular complex determined by the topology of the original MHD equilibrium solution. The topology of plasma configurations is preserved by the transformations

(16). All CGL solutions obtained from non-Beltrami MHD equilibria using Theorem 1 have the same magnetic surfaces as the original MHD equilibrium.

Corollary 1. *Let* $\{\mathbf{B}(\mathbf{r}), P(\mathbf{r})\}$ *be a solution of the static plasma equilibrium system*

$$\operatorname{curl}\mathbf{B}\times\mathbf{B}=\mu\operatorname{grad}P,\qquad \operatorname{div}\mathbf{B}=0. \tag{22}$$

Then $\{\mathbf{B}_1(\mathbf{r}), p_\perp(\mathbf{r}), p_\parallel(\mathbf{r})\}$ *is a solution to static CGL plasma equilibrium system*

$$\left(\frac{1}{\mu}-\tau\right)\operatorname{curl}\mathbf{B}\times\mathbf{B}=\operatorname{grad}p_\perp+\tau\operatorname{grad}\frac{\mathbf{B}^2}{2}+\mathbf{B}(\mathbf{B}\cdot\operatorname{grad}\tau),\qquad \operatorname{div}\mathbf{B}=0, \tag{23}$$

where

$$\begin{aligned}&\mathbf{B}_1(\mathbf{r})=f(\mathbf{r})\mathbf{B}(\mathbf{r}),\\ &p_{\perp1}(\mathbf{r})=C_0\mu P(\mathbf{r})+C_1+\bigl(C_0-f(\mathbf{r})^2/\mu\bigr)\mathbf{B}(\mathbf{r})^2/2,\\ &p_{\parallel1}(\mathbf{r})=C_0\mu P(\mathbf{r})+C_1-\bigl(C_0-f(\mathbf{r})^2/\mu\bigr)\mathbf{B}(\mathbf{r})^2/2.\end{aligned} \tag{24}$$

Remark 3. The above corollary can be directly used to construct a wide variety of anisotropic plasma equilibrium solutions of different topologies. From any harmonic function $f:\nabla^2 f=0$ and using a corresponding vacuum magnetic field $\mathbf{B}=\nabla f$ we can build nondegenerate CGL plasma equilibria.

In Section 4, we present several analytical examples of anisotropic CGL plasma equilibria obtained with the help of the above corollary.

3. Physical conditions and stability of the new solutions

To model real phenomena, any isotropic and anisotropic MHD equilibrium solution has to satisfy natural physical conditions. For solutions in bounded domain $\mathcal{D}$ with boundary $\partial\mathcal{D}$, one should demand

$$\begin{aligned}&0\leqslant p_\parallel|_{\mathcal{D}}\leqslant\mathcal{P}_{\max},\qquad 0\leqslant p_\perp|_{\mathcal{D}}\leqslant\mathcal{P}_{\max},\\ &0\leqslant\mathbf{B}^2|_{\mathcal{D}}\leqslant\mathcal{B}^2_{\max},\qquad 0\leqslant\mathbf{V}^2|_{\mathcal{D}}\leqslant\mathcal{V}^2_{\max},\qquad 0\leqslant\rho|_{\mathcal{D}}\leqslant\rho_{\max},\\ &\mathbf{n}\cdot\mathbf{B}|_{\partial\mathcal{D}}=0,\qquad \mathbf{n}\cdot\mathbf{V}|_{\partial\mathcal{D}}=0\quad\text{or}\quad\mathbf{V}|_{\partial\mathcal{D}}=0.\end{aligned} \tag{25}$$

For an unbounded domain $\mathcal{D}$, the natural conditions are

$$\begin{aligned}&0\leqslant p_\parallel|_{\mathcal{D}}\leqslant\mathcal{P}_{\max},\qquad 0\leqslant p_\perp|_{\mathcal{D}}\leqslant\mathcal{P}_{\max},\\ &0\leqslant\mathbf{B}^2|_{\mathcal{D}}\leqslant\mathcal{B}^2_{\max},\qquad 0\leqslant\mathbf{V}^2|_{\mathcal{D}}\leqslant\mathcal{V}^2_{\max},\qquad 0\leqslant\rho|_{\mathcal{D}}\leqslant\rho_{\max},\\ &p_\parallel,\ p_\perp,\ \mathbf{B}^2,\ \mathbf{V}^2,\ \rho\to\text{const}\quad\text{at }|\mathbf{r}|\to\infty.\end{aligned} \tag{26}$$

For solutions in vacuum, the asymptotic constants must be zero.

If the free functions $f(\mathbf{r})$, $g(\mathbf{r})$ in the transformations (16) are separated from zero, then the transformed anisotropic solutions retain the boundedness of the original solution. The

functions $f(\mathbf{r})$, $g(\mathbf{r})$ in every particular model must be selected so that the new anisotropic solution has proper asymptotics at $|\mathbf{r}| \to \infty$.

Now we address the question of stability of the new equilibrium solutions (16). Under the assumption of double-adiabatic behaviour of plasma (3), it is known that the fire-hose instability takes place when

$$p_\parallel - p_\perp > \mathbf{B}^2/\mu \tag{27}$$

(or, equivalently, $\tau > 1/\mu$), and mirror instability—when

$$p_\perp\left(\frac{p_\perp}{6p_\parallel} - 1\right) > \mathbf{B}^2/2\mu. \tag{28}$$

Now we explicitly check these conditions for the transformed CGL equilibria $\{\mathbf{V}_1(\mathbf{r}), \mathbf{B}_1(\mathbf{r}), p_{\perp 1}(\mathbf{r}), p_{\parallel 1}(\mathbf{r}), \rho_1(\mathbf{r})\}$ (16), supposing that the original isotropic MHD equilibrium configuration $\{\mathbf{V}(\mathbf{r}), \mathbf{B}(\mathbf{r}), P(\mathbf{r}), \rho(\mathbf{r})\}$ satisfies physical conditions (25) or (26).

From (16), for the new solutions

$$p_{\parallel 1} - p_{\perp 1} = \big(1/\mu - C_0/f^2\big)\mathbf{B}_1^2 = \frac{\mathbf{B}^2 f^2}{\mu} - C_0\mathbf{B}^2.$$

Hence the fire-hose instability is not present when

$$\frac{\mathbf{B}^2 f^2}{\mu} - C_0\mathbf{B}^2 \leqslant \frac{\mathbf{B}_1^2}{\mu} = \frac{\mathbf{B}^2 f^2}{\mu}.$$

Thus any choice of $C_0 \geqslant 0$ prevents the new solutions from having the fire-hose instability.

Now we consider the sufficient condition of the mirror instability (28). We define $Q = C_0\mu P(\mathbf{r}) + C_1$, and demand

$$p_{\perp 1}\left(\frac{p_{\perp 1}}{6p_{\parallel 1}} - 1\right) \leqslant \frac{\mathbf{B}_1^2}{2\mu},$$

which rewrites as

$$-\left(5Q + \frac{7}{2}\left(\frac{f^2}{\mu} - C_0\right)\mathbf{B}^2\right)\left(Q - \frac{1}{2}\left(\frac{f^2}{\mu} - C_0\right)\mathbf{B}^2\right) \leqslant \frac{3f^2\mathbf{B}^2}{2\mu}\left(2Q + \mathbf{B}^2\left(\frac{f^2}{\mu} - C_0\right)\right).$$

This is a square inequality with respect to an unknown function $z = f^2(\mathbf{r})$ constant on magnetic field lines and plasma streamlines:

$$\frac{\mathbf{B}^4}{2\mu}z^2 - 4\mathbf{B}^2\big(2Q + C_0\mathbf{B}^2\big)z - \frac{1}{2}\mu\big(10Q - 7C_0\mathbf{B}^2\big)\big(2Q + C_0\mathbf{B}^2\big) \leqslant 0. \tag{29}$$

From this inequality we determine the possible range of $f^2(\mathbf{r})$. If we take $C_1 \geqslant 0$ (and thus $Q \geqslant 0$) and assume $\mathbf{B}^2 > 0$ in the plasma domain, then the discriminant $D = 3\mathbf{B}^4(2Q + C_0\mathbf{B}^2)(14Q + 3C_0\mathbf{B}^2)$ is nonnegative, and the roots are

$$z_{1,2} = \frac{4\mu}{\mathbf{B}^2}\big(2Q + C_0\mathbf{B}^2\big) \mp \frac{\mu\sqrt{D}}{\mathbf{B}^4}. \tag{30}$$

Under the above assumptions of boundedness of P and $\mathbf{B}^2$, in many configurations there may exist ranges of C_0, C_1 such that on every magnetic surface S: $0 < \max_S z_1 < \min_S z_2$. (In the case of static plasma equilibria it is always true, because $P|_S = \text{const} \geqslant 0$, hence $Q|_S = \text{const} \geqslant 0$, and it is easy to check that $z_1|_S(\mathbf{B})$ is always concave down, while $z_2|_S(\mathbf{B})$ is concave up).

The values of $f^2(\mathbf{r})$ on magnetic surfaces must be selected within the interval $\max_S z_1 \leqslant f^2(\mathbf{r})|_S \leqslant \min_S z_2$, and thus the new CGL solution will not have the mirror instability. This is the only limitation on the choice of the function $f^2(\mathbf{r})$.

In Section 4 below, we discuss particular examples and explicitly verify the fire-hose and mirror instability conditions.

Therefore for any MHD equilibrium satisfying necessary physical conditions one can construct infinitely many anisotropic CGL equilibria that are free from fire-hose and mirror instabilities.

4. Examples of anisotropic (CGL) plasma equilibria

4.1. A closed flux tube with no geometrical symmetries

The transformations between isotropic and anisotropic motionless plasmas (24) can indeed be applied to vacuum magnetic field configurations

$$\mathbf{B} = \operatorname{grad} f(\mathbf{r}), \qquad \operatorname{div} \mathbf{B} = 0, \tag{31}$$

which are equivalent to solutions of the Laplace equation $\nabla^2 f(\mathbf{r}) = 0$. Magnetic fields produced by linear electric currents represent a part of this family; they have a critical line coinciding with the line of current and decrease at infinity, according to Bio-Savart law

$$\mathbf{B}(\mathbf{r}) = \frac{\mu I}{4\pi} \int\limits_L \frac{\mathbf{dl} \times (\mathbf{r} - \mathbf{r}_1)}{(\mathbf{r} - \mathbf{r}_1)^3}. \tag{32}$$

Such magnetic fields can have different topologies, depending on the shape of current circuit. For instance, if the current circuit is flat, one readily shows that the magnetic field lines are closed, and therefore lie on magnetic surfaces (which in this case are not defined uniquely).

Such fields themselves represent degenerate plasma equilibria (22) with no pressure and currents, but they can be used for construction of nontrivial CGL plasma equilibria.

In this example we apply the Corollary 1 to a magnetic field produced by a nonsymmetric closed line of current having the parametrization

$$\begin{aligned} &x(t) = 10.0\cos(2\pi t), \qquad y(t) = 7.7\sin(2\pi t), \\ &z(t) = 10.0\big(t^2 - t\big)\sin^2(16\pi t), \end{aligned} \tag{33}$$

where all coefficients have appropriate dimensions so that x, y, z are measured in meters.

It is no analytical representation for a magnetic field from such a circuit. For several starting points, we numerically traced magnetic field lines parameterized by $\mathbf{r}(t)$:

$$\frac{\mathrm{d}\mathbf{r}(t)}{\mathrm{d}t} = \mathbf{B}\big(\mathbf{r}(t)\big), \tag{34}$$

using with Runge–Kutta method of degree 4 ($\mu/4\pi = 1$, $I = 1$).

Fig. 1. Three toroidal magnetic surfaces of an anisotropic flux tube configuration. These surfaces are nested one inside another from the right to the left. They are displayed separately for clear visibility purposes.

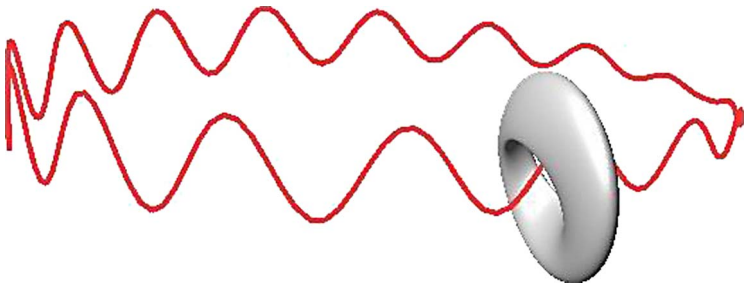

Fig. 2. The mutual position of the current conductor and the boundary of the anisotropic flux tube around it.

For the current conductor configuration (33), the calculations suggest that the magnetic field lies on 2-dimensional nested tori, which were reconstructed using Delaunay triangulation algorithm implemented in `tcocone` software.

The shape of three such nested tori is shown on Fig. 1, whereas the position of one of these tori with respect to the circuit is presented on Fig. 2.

Fig. 3 shows the Poincare section of the dynamical system (34) for the initial data lying on the same three tori.

In this family of nested tori, one can choose a particular torus T_0, and a transverse variable ψ continuously enumerating all the family members inside it, $0 \leqslant \psi < \infty$. For example, one can choose $\psi|_{T_0} = 0$ to correspond to the outmost torus, $\psi \to \infty$ near the axis of the family. Then by Corollary 1 one has an infinite-dimensional set of CGL plasma equilibrium configurations

$$\begin{aligned}
&\mathbf{B}_1(\mathbf{r}) = f(\psi)\mathbf{B}(\mathbf{r}),\\
&p_{\perp 1}(\mathbf{r}) = C_1 + \bigl(C_0 - f(\psi)^2/\mu\bigr)\mathbf{B}(\mathbf{r})^2/2,\\
&p_{\parallel 1}(\mathbf{r}) = C_1 - \bigl(C_0 - f(\psi)^2/\mu\bigr)\mathbf{B}(\mathbf{r})^2/2,\\
&\tau_1(\psi) = 1/\mu - C_0/f(\psi)^2.
\end{aligned} \tag{35}$$

We select the torus on Fig. 1(a) to be the boundary of the plasma domain $\mathcal{D}$. The calculations show that $0.14 < \mathbf{B}^2|_{\mathcal{D}} \leqslant 6.82$.

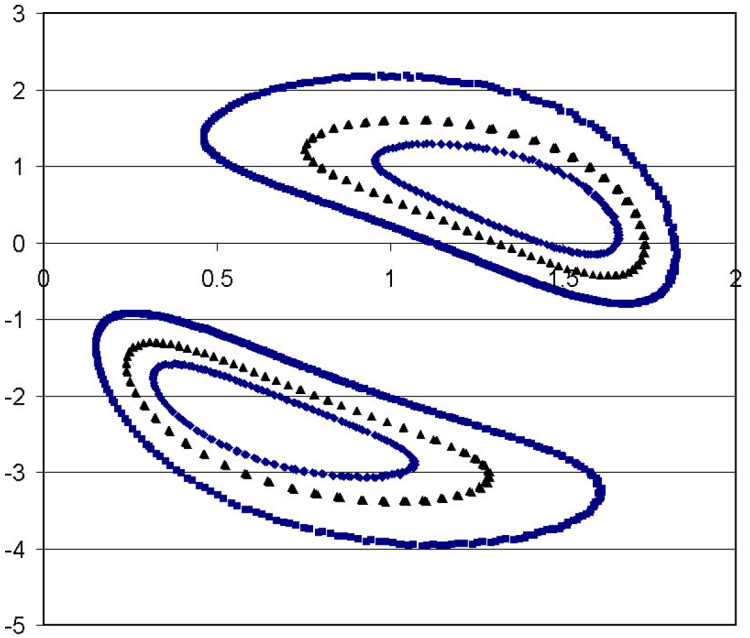

Fig. 3. The Poincare section of the magnetic field lines (dynamical system (34)) lying on three nested magnetic surfaces of the anisotropic flux tube configuration.

We choose now $C_0 = 5, C_1 = 2$. $f(\psi)$ is an arbitrary function defined on the range of ψ; the range of $f(\psi)$ must be chosen so that within the whole plasma domain the mirror instability condition is satisfied (30):

$$\frac{4}{\mathbf{B}^2}\left(2Q + C_0\mathbf{B}^2\right) - \frac{\sqrt{D}}{\mathbf{B}^4} \leqslant \frac{f(\mathbf{r})^2}{\mu} \leqslant \frac{4}{\mathbf{B}^2}\left(2Q + C_0\mathbf{B}^2\right) + \frac{\sqrt{D}}{\mathbf{B}^4}.$$

Using the parameters listed above, this gives

$$4.46 \leqslant \frac{f(\mathbf{r})^2}{\mu} \leqslant 40.24. \tag{36}$$

The requirement for pressure positive-definiteness $p_\parallel \geqslant 0$, $p_\perp \geqslant 0$ is expressed from (24) and gives an additional condition on $f(\mathbf{r})^2$:

$$\mu C_0 - \frac{2C_1}{\mathbf{B}^2} \leqslant f(\mathbf{r})^2 \mu C_0 + \frac{2C_1}{\mathbf{B}^2},$$

which in the given set-up gives

$$4.42 \leqslant \frac{f(\mathbf{r})^2}{\mu} \leqslant 5.58. \tag{37}$$

Finding the intersection of the two ranges (24) and (24), we conclude that all solutions having the range

$$4.46 \leqslant \frac{f(\mathbf{r})^2}{\mu} \leqslant 5.58 \tag{38}$$

satisfy physical conditions for pressure and are not subject to mirror or fire-hose instabilities.

The domain in which the solution is defined is bounded by the torus $\psi = 0$, which is a magnetic surface, therefore everywhere on the boundary $\mathbf{B}_1(\mathbf{r})$ is tangent to it. Hence we may define $\mathbf{B}_1(\mathbf{r}) \equiv 0$ outside of the domain. The discontinuity in tangent component of the magnetic field corresponds to a surface current on the bounding torus

$$\mathbf{i}_b(\mathbf{r}) = \mu^{-1}\mathbf{B}_1(\mathbf{r}) \times \mathbf{n}_1(\mathbf{r}),$$

where $\mathbf{n}_1(\mathbf{r})$ is an outward normal.

The presented exact solutions model a closed flux tube with no geometrical symmetries. The notion of nested flux tubes has been extensively used in theoretical MHD analysis (see, e.g., [18]) and in applications (e.g., a model of a ball lightning as a knotted system of closed force-free flux tubes presented in [20]).

In this family of solutions, as in all solutions built using Theorem 1, the arbitrary function $f(\mathbf{r})$ is a function on a cellular complex which is in this case represented by a closed line segment enumerating the nested toroidal magnetic surfaces from the outmost to the magnetic axis.

4.2. An anisotropic plasma equilibrium with magnetic field dense in a 3D region

We now construct a CGL plasma equilibrium from a magnetic field produced by the same closed current circuit (33) and an additional straight current $I_2 = 3$ in the positive direction of z-axis.

Fig. 4 shows the Poincare section of the dynamical system (34) describing a magnetic field line starting from the point $x = 1.1$; $y = 10.0$; $z = 1.2$. The calculation thus suggests that the magnetic filed line does not lie on any compact magnetic surface, but is dense in some 3D region.

Applying Corollary 1, one gets an anisotropic plasma equilibrium from this pure magnetic field configuration. In this case the topology requirement on the function $f(\mathbf{r})$ is that it must be constant in the whole plasma domain.

4.3. An anisotropic model of helically-symmetric astrophysical jets

Below we present an anisotropic helically-symmetric model of astrophysical jets. It is obtained by application of the Theorem 1 to certain isotropic helically symmetric MHD equilibria.

We start with the following helically symmetric [21] magnetic fields:

$$\mathbf{B}_h = \frac{\psi_u}{r}\hat{\mathbf{e}}_r + B_1\hat{\mathbf{e}}_z + B_2\hat{\mathbf{e}}_\phi, \qquad B_1 = \frac{\alpha\gamma\psi - r\psi_r}{r^2+\gamma^2}, \qquad B_2 = \frac{\alpha r\psi + \gamma\psi_r}{r^2+\gamma^2}, \quad (39)$$

where $\hat{\mathbf{e}}_r$, $\hat{\mathbf{e}}_z$, $\hat{\mathbf{e}}_\phi$ are the unit orts in the cylindrical coordinates r, z, ϕ and $\psi = \psi(r, u)$ is the flux function, $u = z - \gamma\phi$, $\alpha = \text{const}$, $\gamma = \text{const}$. In [7], the exact plasma equilibria (39), $\operatorname{curl}\mathbf{B} \times \mathbf{B} = \mu \operatorname{grad} P$, $\operatorname{div}\mathbf{B} = 0$ were obtained, that correspond to the flux functions

$$\psi_{Nmn} = e^{-\beta r^2}\big(a_N B_{0N}(y) + r^m B_{mn}(y)\big(a_{mn}\cos(mu/\gamma) + b_{mn}\sin(mu/\gamma)\big)\big), \quad (40)$$

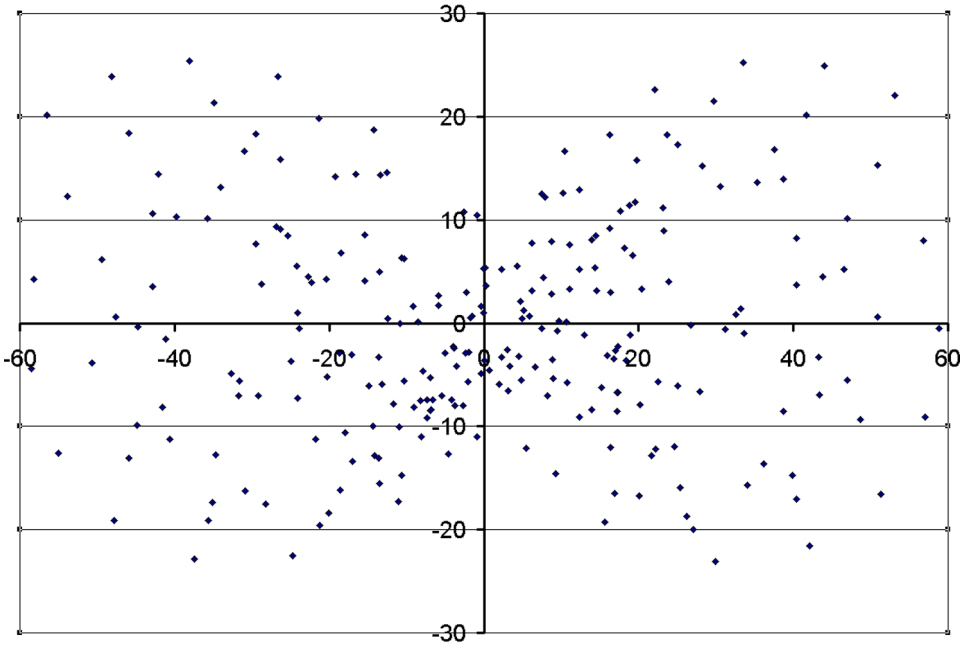

Fig. 4. The Poincare section of a magnetic field line (dynamical system (34)) for another anisotropic plasma configuration (Section 3.2). The figure suggests that this magnetic field line does not lie on a 2D surface.

where N, m, n are arbitrary integers $\geqslant 0$ satisfying the inequality $2N > 2n + m$, and $y = 2\beta r^2$. The plasma pressure is $P = p_0 - 2\beta^2\psi^2/\mu$, and the plasma velocity $\mathbf{V} = 0$. The functions $B_{mn}(y)$ are polynomials [7].

The simplest exact solution (40) is defined for $N = 1, m = 1, n = 0$ and has the form

$$\psi_{110}(r, z, \phi) = e^{-\beta r^2}\big(1 - 4\beta r^2 + a_1 r\cos(z/\gamma - \phi)\big). \tag{41}$$

Applying the symmetry transforms [7] to the exact solutions (39), (40) with $\mathbf{V} = 0$, an infinite family of new field-aligned MHD equilibria was obtained [7]:

$$\mathbf{B}_1 = k\,\mathrm{ch}\,d(\mathbf{r})\mathbf{B}_h, \qquad \mathbf{V}_1 = \frac{k\,\mathrm{sh}\,d(\mathbf{r})}{\sqrt{\mu\rho_1(\mathbf{r})}}\mathbf{B}_h, \qquad P_1 = k^2 P - \frac{k^2}{2\mu}\mathrm{sh}^2 d(\mathbf{r})\mathbf{B}_h^2. \tag{42}$$

Here $d(\mathbf{r})$ and the plasma density $\rho_1(\mathbf{r}) \geqslant 0$ are arbitrary smooth functions that are constant on the magnetic field lines (39), which coincide with plasma streamlines.

We now apply the transformations (16) to the dynamic equilibria (42) and obtain new anisotropic CGL equilibria

$$\begin{aligned}
&\mathbf{B}_a = f(\mathbf{r})\mathbf{B}_1, \qquad \mathbf{V}_a = g(\mathbf{r})\mathbf{V}_1, \qquad \rho_a = C_0\rho_1\mu/g(\mathbf{r})^2,\\
&p_{\perp a} = C_0\mu P_1 + C_1 + \big(C_0 - f(\mathbf{r})^2/\mu\big)\mathbf{B}_1^2/2,\\
&p_{\parallel a}(\mathbf{r}) = C_0\mu P_1 + C_1 - \big(C_0 - f(\mathbf{r})^2/\mu\big)\mathbf{B}_1^2/2,
\end{aligned} \tag{43}$$

and $f(\mathbf{r})$, $g(\mathbf{r})$ are arbitrary functions constant on the magnetic field lines; $C_0 > 0$, C_1 are arbitrary constants.

We note that for this family of solutions magnetic field lines all go to infinity in the variable z [7]. Therefore functions $d(\mathbf{r})$ and $\rho_1(\mathbf{r})$ in the MHD solution (42) and $f(\mathbf{r})$, $g(\mathbf{r})$ in the CGL solution (43) depend on two transversal variables and have no symmetry in general. Hence the generic exact solutions (43) are nonsymmetric.

Let us consider a particular solution from the family (43) in greater detail. We take the flux function ψ_{Nmn} in the simplest form (41), and the arbitrary functions and constants in the form

$$f(\mathbf{r}) = \left(C_0 + 1/\cosh\left(\psi^2\right)\right)^{1/2}, \qquad g(\mathbf{r}) = 0, \qquad C_0 = 1.0, \qquad C_1 = 0.01. \quad (44)$$

This choice corresponds to a static equilibrium.

Fig. 5 shows the section $z = 0$ of the magnetic surfaces $\psi(r, \phi) = \text{const}$ for $a_1 = -1$, $\beta = 0.1$, $\gamma = \sqrt{5/2}$, $\alpha = 3/2\gamma$.

Fig. 6 represents the profiles of pressure along the X-axis (Original isotropic pressure P shown with a thin solid line, anisotropic $p_{\|a}$ with a thick dash line, and $p_{\perp a}$ with a thick solid line). Positive-pressure requirement is evidently satisfied.

On Fig. 7, the original isotropic and the transformed anisotropic magnetic field magnitudes $\mathbf{B}^2$ and $\mathbf{B}_a^2$ along the X-axis are shown (isotropic with a thin solid line, and anisotropic with a thick solid line). The magnetic field is evidently bounded from above, therefore, in accordance with stability considerations presented in Section 3, the presented sample solution is free from fire-hose and mirror instabilities.

On Fig. 8, the cellular complex is shown on which the arbitrary functions $f(\mathbf{r})$, $g(\mathbf{r})$ of the transformations (43) are defined (See Remark 2 in Section 2).

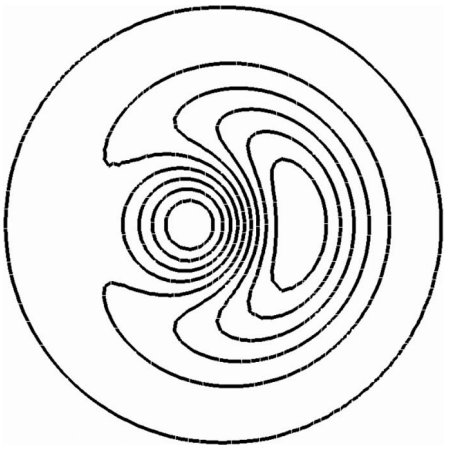

Fig. 5. The section $z = 0$ of the magnetic surfaces $\psi(r, \phi) = \text{const}$ for a helically-symmetric astrophysical jet model ($a_1 = -1$, $\beta = 0.1$, $\gamma = \sqrt{5/2}$, $\alpha = 3/2\gamma$).

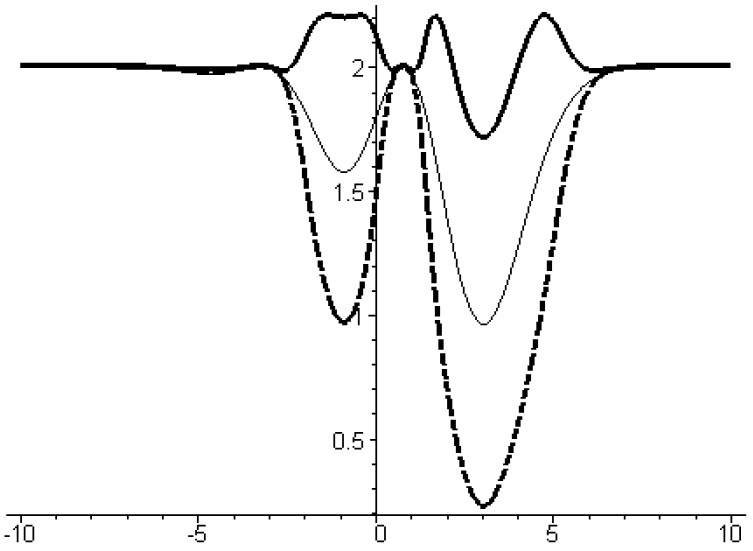

Fig. 6. The profiles of pressure along the X-axis for a helically-symmetric astrophysical jet model ($a_1 = -1$, $\beta = 0.1$, $\gamma = \sqrt{5/2}$, $\alpha = 3/2\gamma$). Original isotropic pressure P is shown with a thin solid line, anisotropic $p_{\|a}$—with a thick dash line, and $p_{\perp a}$—with a thick solid line. Positive-pressure requirement is satisfied.

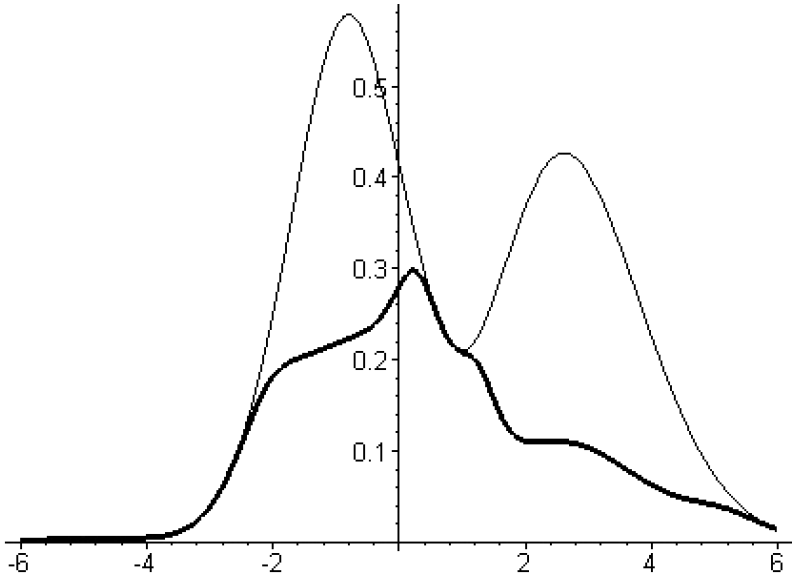

Fig. 7. The magnetic field magnitudes $\mathbf{B}^2$ and $\mathbf{B}_a^2$ for isotropic and anisotropic helically-symmetric astrophysical jet models ($a_1 = -1$, $\beta = 0.1$, $\gamma = \sqrt{5/2}$, $\alpha = 3/2\gamma$) (along the X-axis). Isotropic is shown with a thin solid line, and anisotropic—with a thick solid line.

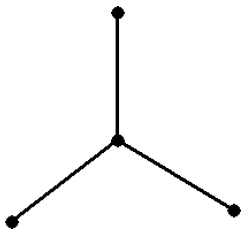

Fig. 8. The cellular complex is shown on which the arbitrary functions $f(\mathbf{r}), g(\mathbf{r})$ are defined (astrophysical jet model solutions (43)).

5. Conclusion

In this paper we present a new method of constructing new anisotropic plasma equilibrium configurations as solutions to the Chew–Goldberger–Low (CGL) system of partial differential equations (7), (8) [2].

The CGL system is a continuum approximation used to describe plasmas in which the mean free path for particle collisions is long compared to Larmor radius, for instance, this is the case in strongly magnetized or rarified plasmas. Unlike isotropic magnetohydrodynamics (MHD) where plasma pressure is a scalar, in the CGL approximation pressure is a tensor with two different components: along the magnetic field $p_{\parallel}$ and in the transverse direction $p_{\perp}$. The Chew–Goldberger–Low system is used to model and study anisotropic plasmas in different areas of physics, such as Earth ionosphere studies [14], plasma confinement [15], and others.

In this paper we considered equilibrium plasma flows and static configurations, which are particularly important in many applications.

In Section 2 we present new infinite-dimensional transformations (16) between isotropic (MHD) and anisotropic (CGL) plasma equilibria. These transformations can be applied to any static plasma equilibrium and to a wide class of dynamic equilibria (those with density ρ constant on plasma streamlines and magnetic field lines) and yield physically interesting anisotropic equilibrium solutions. The result is formulated in Theorem 1, which contains the explicit form of the transformations.

The new anisotropic solutions obtained from these transformations retain the topology of the original isotropic plasma equilibrium solution.

For the solutions of the equations to model the physical reality, they must satisfy natural boundary conditions for a phenomenon under consideration. These constraints are discussed in Section 3, along with another important issue for equilibrium solutions—their stability.

It is shown that if the free functions $f(\mathbf{r})$, $g(\mathbf{r})$ in the transformations (16) are separated from zero, then the transformed anisotropic solutions retain the boundedness of the original solution.

No general methods for proving stability of an MHD or a CGL plasma equilibrium are known; however, there are explicit instability conditions. In Section 3, we also show that the new anisotropic solutions obtained with the help of transformations (16) can be

made free of fire-hose and mirror instability by the proper choice of the transformation parameters.

The examples of using the transformations to construct new anisotropic plasma equilibrium solutions are given in Section 4. The first example is a closed nonsymmetric anisotropic plasma tube spanned by nested toroidal flux surfaces. It is obtained by applying the transformations (16) to a pure magnetic field of a closed thin current conductor.

The second example suggests the existence of static anisotropic nonsymmetric plasma equilibria with magnetic field lines dense in a 3D domain. The exact form of the solution is known; the shape of the magnetic field lines was reconstructed from the dynamical system $d\mathbf{r}/dt = \mathbf{B}(\mathbf{r})$ numerically. The computations suggest the topology mentioned above.

The third example is a model of anisotropic helically-symmetric astrophysical jets. It which is based on the family of solutions for isotropic MHD equations obtained in [7].

The method of constructing anisotropic plasma equilibrium configurations from known isotropic MHD equilibrium solutions presented in this paper can be applied to any static MHD equilibrium or any dynamic incompressible MHD equilibrium with density constant on magnetic field lines and plasma streamlines.

References

[1] B.S. Tahenbaum, Plasma Physics, McGraw-Hill, New York, 1967.
[2] G.F. Chew, M.L. Goldberger, F.E. Low, Proc. Roy. Soc. (A) 236 (1956) 112.
[3] A.S. Bishop, Project Sherwood: The U.S. Program in Controlled Fusion, Addison-Wesley, Reading, MA, 1958.
[4] A. Ferrari, Annual Rev. Astronom. Astrophys. 36 (1998) 539–598.
[5] R.D. Blandford, D.C. Payne, Monthly Notices Roy. Astronom. Soc. 199 (1982) 883.
[6] K.L. Chan, R.N. Henriksen, Astrophys. J. 241 (1980) 534.
[7] O.I. Bogoyavlenskij, Phys. Rev. E. 62 (2002) 8616–8627.
[8] J. Contopoulos, R.V.E. Lovelace, Astrophys. J. 429 (1994) 139.
[9] Y.H. Ohtsuki, H. Ofuruton, Nature 350 (1991) 139.
[10] R. Kaiser, D. Lortz, Phys. Rev. E 52 (3) (1995) 3034.
[11] R. Lust, A. Schluter, Z. Astrophys. 34 (1954) 263.
[12] A.A. Bobnev, Magnitnaya Gidrodinamika 24 (4) (1998) 10.
[13] Ranada, et al., J. Geophys. Res. A 103 (1998) 23309.
[14] B.J. Anderson, et al., J. Geophys. Res. 99 (1994) 5877.
[15] H. Yamada, et al., Nuclear Fusion 32 (1992) 25.
[16] O.I. Bogoyavlenskij, Phys. Lett. A 291 (4–5) (2001) 256–264.
[17] O.I. Bogoyavlenskij, Phys. Rev. E 66 (2002).
[18] H.K. Moffatt, Vortex- and magneto-dynamics—A topological perspective, in: Mathematical Physics 2000, Imperial College, London, 2000, p. 170.
[19] M.D. Kruskal, R.M. Kulsrud, Phys. Fluids 1 (1958) 265.
[20] Ranada, et al., J. Geophys. Res. A 103 (1998) 23309.
[21] J.L. Johnson, C.R. Oberman, R.M. Kulsrud, E.A. Frieman, Phys. Fluids 1 (1958) 281.